

Electron properties of a system of two-parameter long-range impurity states

M. A. Ivanov and Yu. G. Pogorelov

Institute of Metal Physics, Academy of Sciences of the Ukrainian SSR

(Submitted 25 September 1984)

Zh. Eksp. Teor. Fiz. **88**, 1738–1751 (May 1985)

The electron properties are studied for semiconductor crystals containing impurity states close to the edge of a band. The states are described by two independent parameters—their energy and their interaction with the continuous spectrum excitations, and the corresponding wave functions are characterized by two radii. The electron excitation spectrum and state density are found by treating both the hybridization between localized and band states and the Coulomb interaction (both between impurities and for a single impurity atom), and phase diagrams are plotted for various relative values of the parameters. It is shown that the properties of two-parameter long-range states are much more diverse than the usual hydrogen-like states described by the effective mass approximation.

1. INTRODUCTION

Long-range impurity states in semiconductor crystals can greatly alter the crystal properties. For example, the Mott transition¹ occurs at impurity concentrations

$$n = n_M = \eta_M a^{-3}, \quad a = \chi \hbar^2 / m e^2, \quad (1)$$

for ordinary hydrogen-like states and is found to be accompanied by metallic conduction at temperature $T = 0$. Here a is the effective Bohr radius, m is the effective mass, χ is the static dielectric permittivity of the crystal, and $\eta_M \approx 0.02$. However, the energy of the hydrogen-like states and their mutual interaction are both described by a single parameter, which greatly limits the range of possible behavior.

On the other hand, there are many long-range impurity states which (unlike hydrogen-like states) require two independent parameters for their description (this is the case, e.g., in the Anderson model). Their wave functions are thus characterized by two radii—a large radius $r_0 = \hbar(2m|\varepsilon_0|)^{-1/2}$ that depends on the distance ε_0 from the impurity level to the nearest band-edge, and a small radius, equal to the atomic radius (or to the Bohr radius for heavy atoms of mass $M \gg m$). Such two-parameter states (TPS) may occur in semiconductors with deep transition-metal impurity states² or when the carrier masses are very different.^{3,4} The one-electron approximation was used in Ref. 5 to study the spectrum for various TPS concentrations in the hybrid s - d Anderson model. However, both the spectrum and the other electron properties of the system can change greatly if one allows for the Hubbard repulsion at the impurity centers and treats the long-range Coulomb interaction between the impurities. In this case, it is essential to analyze the relative importance of the effects associated with hybridization and Coulomb interaction. The phase diagram for the electron properties of crystals with two-parameter states is thus much richer and more diverse than for the simple hydrogen-like states. For example, hybridization can suppress the conductivity as the impurity concentration increases, so that metallic and dielectric phases may alternate when an external parameter (e.g., the pressure) is steadily increased. In addition, Wigner crystallization can occur in both the metallic and dielectric phases.

In Sec. 2 we will examine the behavior of a system containing a high concentration ($n \gg r_0^{-3}$) of neutral TPS-forming impurities; the electron concentration in the states is assumed to be low, $\tilde{n} \ll n$. The case of completely filled donor (or acceptor) two-parameter states ($\tilde{n} = n$) is analyzed in Secs. 3 and 4 for various relative values of the hybridization and Coulomb interaction parameters. We assume throughout that the Hubbard repulsion parameter $U \rightarrow \infty$.

2. ELECTRON SPECTRUM OF A CRYSTAL WITH A HIGH IMPURITY CONCENTRATION FOR NEARLY EMPTY IMPURITY STATES

As in Ref. 5, we will use the hybrid s - d Anderson model⁶ to analyze the electron excitation spectrum of crystals containing impurities. The Hamiltonian is

$$H = \sum_{\mathbf{k}, \sigma} \varepsilon_{\mathbf{k}} a_{\mathbf{k}\sigma}^+ a_{\mathbf{k}\sigma} + \varepsilon_d \sum_{\mathbf{p}, \sigma} b_{\mathbf{p}\sigma}^+ b_{\mathbf{p}\sigma} + \frac{1}{\sqrt{V}} \sum_{\mathbf{k}, \mathbf{p}, \sigma} (\gamma_{\mathbf{k}} e^{i\mathbf{k}\cdot\mathbf{p}} a_{\mathbf{k}\sigma}^+ b_{\mathbf{p}\sigma} + \text{h.c.}) + U \sum_{\mathbf{p}} n_{\mathbf{p}\uparrow} n_{\mathbf{p}\downarrow}. \quad (2)$$

Here σ is the electron spin; $a_{\mathbf{k}\sigma}^+$ and $a_{\mathbf{k}\sigma}$ are the annihilation and creation operators for the band states of energy $\varepsilon_{\mathbf{k}} = \hbar^2 k^2 / 2m$; $b_{\mathbf{p}\sigma}^+$ and $b_{\mathbf{p}\sigma}$ are the corresponding impurity state operators (the impurity states, of energy ε_d , are assumed to be nondegenerate); the vector \mathbf{p} labels the lattice sites that contain impurities; $n_{\mathbf{p}\sigma} = b_{\mathbf{p}\sigma}^+ b_{\mathbf{p}\sigma}$; $\gamma_{\mathbf{k}}$ is the hybridization parameter; V is the volume of the crystal; $U > 0$ is the intraatomic Coulomb repulsion parameter for the impurities and may be assumed to be larger than any other parameter of the system.

In this section we will consider acceptor impurity centers whose renormalized energy

$$\bar{\varepsilon}_d = \varepsilon_d - V^{-1} \sum_{\mathbf{k}} |\gamma_{\mathbf{k}}|^2 / \varepsilon_{\mathbf{k}}$$

lies near the bottom of the conduction band. The energy of an extra electron localized at an isolated impurity is then found by solving the equation

$$D(\varepsilon) = \varepsilon - \bar{\varepsilon}_d - \frac{1}{4\pi} \left(\frac{2m}{\hbar^2} \right)^{3/2} \gamma^2 \sqrt{\varepsilon - \varepsilon_d} = 0 \quad (3)$$

(we will henceforth assume that the symmetry of the band and impurity states is such that $\gamma^2 \equiv |\gamma_{\mathbf{k} \rightarrow 0}|^2 \neq 0$). Equation (3) has the solution

$$\varepsilon_0 = \bar{\varepsilon}_d - \frac{\varepsilon_t}{2} [1 - (1 - 4\bar{\varepsilon}_d/\varepsilon_t)^{1/2}], \quad \varepsilon_t = \frac{(2m)^3 \gamma^4}{(4\pi)^2 \hbar^6}, \quad (4)$$

which is sensitive to the ratio $\bar{\varepsilon}_d/\varepsilon_t$, where ε_t is the width of the "threshold" region. Far from the impurity center, this state has the wave function (for $\varepsilon_0 < 0$)

$$\psi(r) = \frac{\psi_0}{(4\pi r_\gamma)^{1/2}} \frac{e^{-r/r_0}}{r}, \quad \psi_0^2 = \left(1 + \frac{r_0}{2r_\gamma}\right)^{-1}, \quad r_\gamma^2 = \frac{\hbar^2}{2m\varepsilon_t}. \quad (5)$$

a) Assume that $\bar{\varepsilon}_d$ exceeds the threshold energy, $|\bar{\varepsilon}_d| \gg \varepsilon_t$. Then $\varepsilon_0 \approx \bar{\varepsilon}_d$, and the wave function is concentrated mostly at the impurity; only a small fraction $\sim r_0/2r_\gamma \ll 1$ of the electron density described by Eq. (5) is distributed in a volume $\sim r_0^3$. This type of distribution corresponds to the structure of the two-parameter states.

It was shown in Ref. 5 that in the one-electron approximation, the spectrum undergoes a coherent rearrangement for high TPS concentrations

$$n \gg n_0 = (3\pi^2 r_0^3)^{-1}. \quad (6)$$

Some of the states near the local level ($\varepsilon_0 < 0$) are then delocalized; these states lie opposite the states in the principal (conduction) band, i.e., on the other side of ε_0 . Their energies are determined by the wave vector; like the energies for states in the band, they obey the dispersion equation

$$\varepsilon - \varepsilon_{\mathbf{k}} - \text{Re } R(\varepsilon) = 0, \quad R(\varepsilon) = n\gamma^2 \left[\varepsilon - \varepsilon_0 - \frac{\gamma^2}{V} \sum_{\mathbf{k}} (\varepsilon - \varepsilon_{\mathbf{k}} - R(\varepsilon))^{-1} \right]^{-1} \quad (7)$$

and they are of the form

$$\varepsilon_{1\mathbf{k}} = \{\varepsilon_{\mathbf{k}} + \varepsilon_0 - [(\varepsilon_{\mathbf{k}} - \varepsilon_0)^2 + 4n\gamma^2]^{1/2}\}/2. \quad (8)$$

The Ioffe-Regel condition, which is equivalent to

$$\varepsilon - \text{Re } R(\varepsilon) > \text{Im } R(\varepsilon), \quad (9)$$

determines the maximum length of the wave vector in this band. The impurity band (8) is thus bounded by

$$n_\gamma^{1/2} (1 + |\varepsilon_0|/\Delta) \sim k_{\min}^{(4)} < k < k_{\max} \sim n^{1/2}, \quad (10)$$

where $n_\gamma = r_\gamma^{-3}$ and

$$\Delta = \varepsilon_0 - \varepsilon_{1\mathbf{k}=0} = [(\varepsilon_0^2 + 4n\gamma^2)^{1/2} - |\varepsilon_0|]/2 \quad (11)$$

is its width. For a specified σ , the density of states in the band is given by

$$\rho_1(\varepsilon) = \frac{1}{2} \rho_0 \left(\varepsilon - \frac{n\gamma^2}{\varepsilon - \varepsilon_0} \right) \left[1 + \frac{n\gamma^2}{(\varepsilon - \varepsilon_0)^2} \right], \quad \rho_0(\varepsilon) = \frac{1}{2\pi^2} \left(\frac{2m}{\hbar^2} \right)^{3/2} \bar{v} \varepsilon. \quad (12)$$

This expression is valid for $\Delta > \varepsilon_0 - \varepsilon \gg \Delta_0$, where $\Delta_0 = n^{1/3} n_\gamma^{1/3} \hbar^2/2m$ is comparable in order of magnitude to the concentration broadening of the impurity level. Elsewhere, the states are localized (out to the renormalized edge of the principal band); their density is determined primarily

by the state density for pairs of neighboring impurities and is given by

$$\rho_2(\varepsilon) = \rho_\tau(\varepsilon) = 2\pi n \Delta_0^3 / (\varepsilon - \varepsilon_0)^4, \quad \gamma^2 m / \hbar^2 a_0 \gg |\varepsilon - \varepsilon_0| \gg \Delta_0, \quad |\varepsilon_0| \gg \varepsilon_t, \quad (13)$$

where a_0 is the lattice constant of the crystal. The dispersion law in the principal band also follows from (7):

$$\varepsilon_{2\mathbf{k}} = \{\varepsilon_{\mathbf{k}} + \varepsilon_0 + [(\varepsilon_{\mathbf{k}} - \varepsilon_0)^2 + 4n\gamma^2]^{1/2}\}/2, \quad (14)$$

and is valid [cf. (9)] for

$$k > k_{\min}^{(2)} \sim n_\gamma^{1/2} (1 + |\varepsilon_0|/\Delta)^{-1}. \quad (15)$$

If the impurity level lies within the continuous spectrum ($\varepsilon_0 > 0$), the state density function will have a well-defined quasilocal peak for $\bar{\varepsilon}_d \gg \varepsilon_t$. For high impurity concentrations $n \gg n_0$, coherent rearrangement occurs and the original spectrum splits into lower and upper branches which obey the dispersion relations (8) [$k_{\min}^{(2)} < k < k_{\max}$] and (14) [$k_{\min}^{(1)} < k$], respectively. Expression (12) remains valid for the density of states for these branches. The states are localized in a quasigap that forms between the upper and lower frequencies ε_0 and $\varepsilon_1 = \varepsilon_0 + \Delta$ of the lower and upper branches; the state density here is determined by the levels of the impurity pairs and is given by Eq. (13). Figure 1 shows the general form of the state density functions $\rho(\varepsilon)$ during coherent spectral rearrangement for the local and quasilocal impurity levels. We note that a second peak is present near $\varepsilon_1 = \varepsilon_0 + \Delta$ for the quasilocal level when $n \ll n_0^{4/3}/n_\gamma^{1/3}$; its height is $\sim n_0/\Delta$, substantially greater than the unperturbed state density $\rho_0(\varepsilon_1)$, and its integrated intensity (area) is $\sim n_0$. Expressions (12) and (13) thus describe $\rho(\varepsilon)$ for a wide range of energies; one or the other of them is valid everywhere outside $|\varepsilon - \varepsilon_0| \lesssim \Delta_0$ (where the impurity level is concentration-broadened) and the narrow transition regions of width $\Delta_{1,2} = |\varepsilon_{1,2k_{\min}} - \varepsilon_{1,2k=0}|$ near the renormalized band edges, where a transition occurs from localized to band states.⁷ The peak in ρ near ε_0 has area $\sim n$ and is asymme-

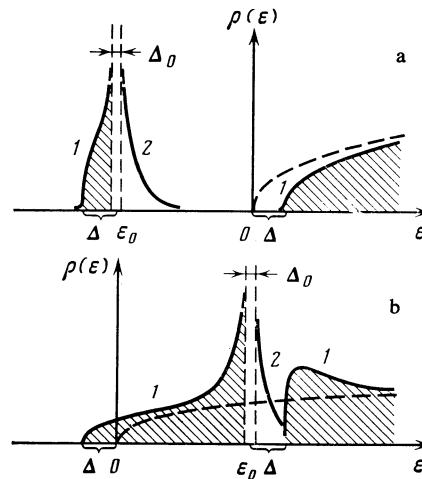


FIG. 1. Density of states at high impurity concentration: a) $\varepsilon_0 < 0$; b) $\varepsilon_0 > 0$. The states in the hatched regions are described by their wave vectors; lines 1 and 2 plot the distributions given by (12) and (13), respectively.

tric— $\rho(\varepsilon) \propto (\varepsilon - \varepsilon_0)^{-4}$ for the localized states, while $\rho(\varepsilon) \propto (\varepsilon - \varepsilon_0)^{-5/2}$ for the band states.

b) We now consider what happens when $\tilde{\varepsilon}_d$ lies in the threshold region, $|\tilde{\varepsilon}_d| \ll \varepsilon_t$. Then if $\tilde{\varepsilon}_d < 0$, a local level of energy $\varepsilon_0 \approx -\tilde{\varepsilon}_d^2/\varepsilon_t$ forms at an isolated impurity (a virtual level forms if $\tilde{\varepsilon}_d > 0$). An “incoherent” spectral rearrangement occurs in this case if $n \gg n_0$; the widths $\Delta_{1,2}$ and Δ_0 of the transition and concentration-broadening intervals then become comparable and are much greater than $|\varepsilon_0|$. No new band (for quasigap) of coherent impurity states is then formed.

However, for high impurity concentrations $n > \tilde{n}_\gamma$, where

$$\tilde{n}_\gamma = \eta_\gamma n_\gamma, \quad \eta_\gamma \approx 1/20, \quad (16)$$

coherent spectral rearrangement and splitting can occur even in this situation; the two branches are then described by a quasimomentum. The corresponding solutions of Eq. (7) are similar to the ones considered above for $n \gg n_0^{4/3}/n_\gamma^{1/3}$. The numerical coefficient η_γ , estimated in Ref. 9 on the basis of a self-consistent analysis, agrees quite closely with the experimental data¹⁰ on light absorption by antiferromagnetic materials containing impurities.

c) The concentration broadening Δ_0 associated with hybridization is not the only mechanism that can spread out the energies of the impurity levels; Coulomb interactions can also cause broadening. We will therefore investigate how inhomogeneous broadening influences the coherent spectral rearrangement. The polarization operator $R(\varepsilon)$ is then of the form

$$R(\varepsilon) = n\gamma^2 \int \frac{P(\varepsilon' - \varepsilon_0)}{\varepsilon - \varepsilon'} d\varepsilon', \quad (17)$$

where the distribution function $P(x)$ describes the diagonal disorder, as in Ref. 10. We assume that the width Γ of the distribution is greater than Δ_0 . The density of localized states near ε_0 is then given by $nP(\varepsilon - \varepsilon_0)$ as long as the latter is greater than $\rho_2(\varepsilon)$. As before, condition (9) determines the nature of the solution of Eq. (7). If $\Gamma \ll \Delta$ then (9) implies that the coherent rearrangement is qualitatively the same as before; however, the maximum wave vector is not determined by

$$|\varepsilon_0 - \varepsilon_{k_{max}}| \sim n\gamma^2/\Gamma, \quad (18)$$

and the specific form of decay of $P(x)$ determines the minimum wave vector. However, if $\Gamma \gg \Delta$ then coherent rearrangement is suppressed; no band states form near the local level, and the quasigap near the quasilocal level disappears. We note that in the latter case, the energy spreading of the levels facilitates delocalization instead of the more usual localization.

d) One might expect that the impurity band of delocalized states that forms during coherent spectral rearrangement would give rise to metallic conduction when the band is filled with electrons. However, because of the large width of the region of localized states this is not always true. We will consider the onset of metallic conduction (at $T = 0$) in more detail for a system containing acceptor impurities with $\varepsilon_0 < 0$ and $n \gg n_0$. We will assume that the levels are filled by electrons provided by additional donor impurities of concentra-

tion $\tilde{n} \ll n$. The concentration \tilde{n} must not be too low, because the Fermi level ε_F must lie within the region of delocalized states of energy ε_{1k} [this will at least ensure that all the localized states of energy $< \varepsilon_{1k_{min}}$ (below the mobility threshold) will be filled]. This yields the inequalities

$$\begin{aligned} \tilde{n} &> \frac{3\pi^2 n_0^2}{32 n}, \quad n \ll \frac{n_0^{4/3}}{n_\gamma^{1/3}}, \\ \tilde{n} &> \frac{1}{12\sqrt{\pi}} n^{1/3} n_\gamma^{1/2}, \quad n \gg \frac{n_0^{4/3}}{n_\gamma^{1/3}} \end{aligned} \quad (19)$$

[we have assumed that the density $\rho_2(\varepsilon)$ of paired levels (13) determines the density of localized states for $\varepsilon < \varepsilon_{1k_{min}}$]. On the other hand, ionized donor centers are present which give rise to a random Coulomb field at the majority impurity centers which discourages delocalized states. Thus, an electron leaving a donor can enter a delocalized state only if the energy gained by localization is less than the bandwidth (11): $\Delta\varepsilon \sim n^{1/3} n_M^{1/3} \hbar^2/2m < \Delta$. If this condition is satisfied, the electron will not be trapped by the acceptors adjacent to the donor (within a distance of $\sim n^{-1/3}$). We thus get

$$\begin{aligned} n &> \pi \left(\frac{3}{2\eta_M} \right)^{1/2} n_0 \left(\frac{n_M}{n_\gamma} \right)^{1/2}, \quad n \ll \frac{n_0^{4/3}}{n_\gamma^{1/3}}, \\ n &> \frac{16}{9\pi\eta_M^2} \frac{n_M^2}{n_\gamma}, \quad n \gg \frac{n_0^{4/3}}{n_\gamma^{1/3}}. \end{aligned} \quad (20)$$

The coefficients were found from the requirement that

$$\int_{-\infty}^{\varepsilon_0 - \Delta} \rho_c(\varepsilon) d\varepsilon = \tilde{n}, \quad \rho_c(\varepsilon) = \frac{4\pi n \tilde{n}}{(\varepsilon - \varepsilon_0)^4} \left(\frac{e^2}{\kappa} \right)^3,$$

where $\rho_c(\varepsilon)$ is the density of Coulomb states.

The above requirements in c) are automatically satisfied if (19) and (20) hold, and the screening radius in this case is found to exceed the average distance between the donors. Metallic conduction can thus occur when (19), (20) hold.

We will now examine which types of impurity centers that give rise to two-parameter states can satisfy (20). Assume first that the carriers in the semiconductor have widely different masses ($m \ll M$). The smaller (r_1) of the two radii characterizing the impurity state in this case is still much greater than the lattice constant; the behavior over distances $\gtrsim r_1$ can therefore be described in terms of the dielectric susceptibility, and in the effective mass approximation the energy of the impurity level^{3,4} is determined primarily by the band for the heavy carriers of mass M . The parameter describing the interaction between the two-parameter states and the light carriers can then be estimated directly as

$$\gamma = 4\beta \hbar e / (\pi \kappa M)^{1/2} \quad (21)$$

in the limit $m/M \rightarrow 0$. Here β is the overlap integral for the Bloch functions at the extremal points for the light- and heavy-carrier bands. The characteristic concentration is thus given by

$$n_* = \left(\frac{4\beta}{\pi} \frac{m}{M} \right)^6 \frac{n_M'}{\eta_M} = \left(\frac{4\beta}{\pi} \right)^6 \frac{n_M}{\eta_M} \left(\frac{m}{M} \right)^3 \ll n_M, \quad (22)$$

where n'_M and n_M are the Mott concentrations for heavy- and light-carrier bands, respectively. The second constraint in (20) is easily seen to determine the minimum TPS concentration for onset of metallic conduction when the position of the impurity level changes relative to the edge of the light-carrier band. Substituting (22) into (20), we find that

$$n > \xi n'_M, \quad \xi = \pi^5 / 2304 \eta_M \beta^6 \approx 7 / \beta^6. \quad (23)$$

Even in the most favorable case $\beta \sim 1$, the lower bound (23) is of the same order of magnitude as the familiar Mott bound for the heavy-carrier band. Thus, if r_1 (the smaller of the two TPS radii) can be described in the effective mass approximation, the impurity band cannot support steady metallic conduction. However, such conduction can occur if r_1 is comparable to the atomic radius. The concept of dielectric permittivity breaks down at atomic dimensions and the parameter γ exceeds the bound determined by (22), so that (20) can be satisfied. The formation of delocalized states in the impurity band can also be observed by injecting external carriers into the system.

3. METALLIC AND DIELECTRIC STATES OF A SYSTEM OF DONOR TWO-PARAMETERS STATES ($\tilde{n}_\gamma \gg n_M$)

We will now analyze what happens when the TPS is a filled donor level near the bottom of the conduction band (or an empty acceptor near the edge of the valence band); each impurity atom is assumed to trap a single electron. We will investigate the electron states of such a system for several impurity concentrations and energies ε_0 (i.e., n and n_0 will be varied). The constant parameters determining the behavior of the system are n_M and n_γ , and strong hybridization will be assumed in this section: $\tilde{n}_\gamma \gg n_M$. We will therefore generally neglect the Coulomb interaction between electrons located at different lattice sites.

a) We first consider an impurity level lying below the bottom of the band: $\varepsilon_0 < 0$. Because of the strong Hubbard repulsion U , at most n electrons can be put into the impurity band. The electron spin will have a definite projection σ at any given impurity site; to fourth order in γ , the spin interaction for $n \ll n_0$ is described by the effective spin Hamiltonian

$$H_{\text{eff}} = \sum_{\mathbf{p}, \mathbf{p}'} I(|\mathbf{p} - \mathbf{p}'|) \sigma_{\mathbf{p}} \sigma_{\mathbf{p}'}, \quad I(r) = \frac{8\varepsilon_t r_0 e^{-2r/r_0}}{r(1+r_0/2r_1)}. \quad (24)$$

Here $\sigma_{\mathbf{p}}$ is the electron spin operator for impurity site \mathbf{p} and is given by the Pauli matrices. Expression (24) was derived in Ref. 11 for $|\varepsilon_0| \gg \varepsilon_t$, which corresponds to $n_0 \gg n_\gamma$. Because of the antiferromagnetic nature of the interaction $I(r)$, the electron system enters a spin glass state at low temperatures $T_f \sim I(n^{-1/3})$ for $n \ll n_0$. For high concentrations $n_0 \ll n \ll \tilde{n}_\gamma$, for which no coherent spectral rearrangement takes place, the transition to the spin glass state occurs at $T_f \sim (n/n_\gamma)^{1/3} \varepsilon_t$. Equation (24) continues to describe the exchange interaction between the impurities for $n \ll n_0^{4/3}/n_\gamma^{1/3}$ when coherent rearrangement occurs, and the transition temperature is

$$T_f \sim \left(n \int I^2(r) d\mathbf{r} \right)^{1/2} \sim (n/n_0)^{1/2} \varepsilon_t.$$

Finally, we obtain $T_f \sim (n/n_\gamma)^{1/8} \varepsilon_t$ if $n \gg \max(\tilde{n}_\gamma, n_0^{4/3}/n_\gamma^{1/3})$.

We will assume that the temperature is high: $T \gg T_f$ in the following analysis of spectral rearrangement and phase transitions.

Because of the hybridization, the density of localized states has a high-frequency tail for small impurity concentrations; this tail is described by (13) if $n_0 \gg n_\gamma$. The electrons from states in the tail with energies $> \varepsilon_{2k=0}$ go into states in the band or else enter hydrogen-like Coulomb states of energy $\varepsilon_R = \hbar^2/2ma$ (the effective Rydberg energy). These electrons thus determine the Fermi level; if their concentration $n'(\varepsilon_{2k=0})$ exceeds n_M and $(k_{\min}^{(2)})^3$, then ε_F lies above the mobility threshold for the principal band and the system becomes metallic. Here n' is given by

$$n'(\varepsilon) = \int_{\varepsilon}^{\infty} \rho_\tau(\varepsilon') d\varepsilon' = \frac{2\pi}{3} \frac{n\Delta_0^3}{(\varepsilon - \varepsilon_0)^3}, \quad \varepsilon > \varepsilon_0, \quad (25)$$

$$n'(\varepsilon_{2k=0}) = \frac{2}{(3\pi)^3} \left(\frac{n}{n_0} \right)^2 n_\tau.$$

The transition to the metallic phase occurs for concentrations $n \gg \tilde{n}_0 (n_M/n_\gamma)^{1/2}$, where

$$\tilde{n}_0 = (1/3\pi^2) (2m|\varepsilon_d|/\hbar^2)^{3/2}.$$

If $n_0 \gg n_\gamma$ and n is increased further to $n \gg n_0$, a region of delocalized states of energies $< \varepsilon_0$ ($\ll \varepsilon_F$) forms as discussed in Sec. 2 and can alter the hole excitation spectrum. For $n_0 \ll n \ll n_0^{4/3}/n_\gamma^{1/3}$, perturbation theory gives the dispersion law

$$\varepsilon_{k\sigma}^{(4)} = \left| \varepsilon_0 - \frac{\gamma^2}{V} \sum_{\mathbf{k}'} \frac{1 - p_\sigma n V/N}{|\varepsilon_0 + \varepsilon_{\mathbf{k}'}} - \frac{p_\sigma n \gamma^2}{|\varepsilon_0 + \varepsilon_{\mathbf{k}}}} \right| \quad (26)$$

to second order in γ . Here p_σ is the relative number of electrons with spin σ and N is the number of lattice sites. The range of validity of (26) is again given by condition (10), with n replaced by $p_\sigma n$. The same procedure can be used to derive the dispersion law

$$\varepsilon_{k\sigma}^{(2)} = \varepsilon_{\mathbf{k}} + p_\sigma n \gamma^2 / (|\varepsilon_0| + \varepsilon_{\mathbf{k}}), \quad (27)$$

for the electrons in the renormalized principal band for all $n \ll n_0^{4/3}/n_\gamma^{1/3}$; Eq. (27) is valid if (15) is satisfied (with n replaced by $p_\sigma n$).

The results (26), (27) show that to second order in γ , the system behaves as if it consisted of two independent subsystems with different spins σ and impurity concentrations $p_\sigma n$. Moreover, (27) implies that the system should have a preferred polarization if more electrons are added to a doping concentration $n_d \gtrsim n_f = 2T_f \varepsilon_0 / \gamma^2$. Preferential spin polarization can occur even without additional doping if $n_0 (n_M/n_\gamma)^{1/2} \ll n \ll n_0$, because in this case n' in (25) may exceed n_f .

One can show quite generally that

$$\varepsilon_{k\sigma}^{(1,2)} = \mp \{ \varepsilon_{\mathbf{k}} + \varepsilon_0 \mp [(\varepsilon_{\mathbf{k}} - \varepsilon_0)^2 + 4p_\sigma n \gamma^2]^{1/2} \} / 2 \quad (28)$$

whenever coherent rearrangement occurs; here the $+$ and $-$ signs correspond to excited electrons and holes, respectively. This result reduces to (27), (26) when $n \ll n_0^{4/3}/n_\gamma^{1/3}$. Finally, we observe that the spectra (26), (28) may have hole branches for $n \gg n_0$, because their width $|\varepsilon_{\mathbf{k}}^{(1)} - \varepsilon_0|$ is $> T_f$.

b) We will next analyze an impurity level lying within the continuous spectrum ($\varepsilon_0 > 0$). We have already noted that in this case, the band spectrum splits for $n \gg n_0$ and a "forbidden" region forms, so that in principle the system can behave like a dielectric if the Fermi level lies in the region of localized states. It is thus very important to determine the maximum number of electrons that can be contained in the lower subband. We begin with the simplest case of completely polarized electrons, for which the dispersion equations (8) and (14) are valid. The number of states with a specified polarization in the upper subband is then independent of the impurity concentration and is exactly equal to the number of states in the band for a perfect crystal, i.e.,

$$\int_{\varepsilon_0+\Delta}^{\varepsilon_{\max}} \rho_1(\varepsilon) d\varepsilon = \frac{1}{2} \int_0^{\varepsilon_{\max}} \rho_0(\varepsilon) d\varepsilon. \quad (29)$$

Since doping increases the number of degrees of freedom in the system by n , the total number of states of the specified polarization in the lower subband [including the contribution from the fluctuation tail in $\rho_2(\varepsilon)$] is precisely equal to n . As the impurities fill up with electrons (for $n_0 \gg n_\gamma$), roughly $n_0/2$ of the electrons are delocalized, and an equal number of impurity sites are empty on the average. The latter sites are responsible for the spectral rearrangement of the electrons with the opposite polarization. According to the above argument, the number of states in the lower subband with the opposite polarization is also equal to $n_0/2$. According to the previous discussion in a), the total number of possible states in the lower subband for both polarizations is then

$$\begin{aligned} n_1 &= n + n_0/2, & \varepsilon_0 > 0, \\ n_1 &= n, & \varepsilon_0 < 0. \end{aligned} \quad (30)$$

The same result clearly follows for an arbitrary degree of polarization in the limit $\gamma \rightarrow 0$. Since the hybridization Hamiltonian does not mix states of different polarization, (30) should be exact (recall that $U \rightarrow \infty$) for arbitrary γ and p_σ . If we assume that the subsystems with different polarizations are independent, as was the case for $\varepsilon_0 < 0$, we can derive the dispersion equation

$$\varepsilon_{k\sigma}^{(1,2)} = \{\varepsilon_k + \varepsilon_0 \pm [(\varepsilon_k - \varepsilon_0)^2 + 4\gamma^2(p_\sigma n + (1-p_\sigma)n_0)]^{1/2}\} / 2 \quad (31)$$

for electron and hole excitations characterized by a quasimomentum.

In order for the Fermi level of a system with n (intrinsic) electrons to lie inside the quasigap for $n \gg n_0$, n_γ and $\varepsilon_0 > 0$, i.e., in order for the system to behave as a dielectric, fewer than $n_0/2$ of the fluctuation states within the upper subband must be unoccupied. That is, we must have $n'(\varepsilon_1) < n_0/2$, where ε_1 is the bottom of the lower of the two upper (spin-split) bands. The Fermi energy, ε_F is then given by

$$n'(\varepsilon_F) = n_0/2, \quad (32)$$

whence

$$\varepsilon_F = \varepsilon_0 + (4\pi/3) n^{2/3} (n_\gamma/n_0)^{1/3} \hbar^2/2m.$$

If ε_F is greater than ε_1 , the Fermi level will lie inside the upper subband near ε_1 and the system will conduct like a metal. The insulator-metal transition for polarization

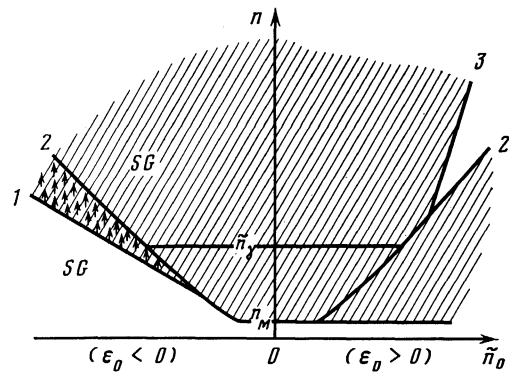


FIG. 2. Phase diagram in the n, \tilde{n}_0 plane for $\tilde{n}_\gamma \gg n_M$. The regions of metallic phase are hatched; the vertical arrows indicate the region of ferromagnetically ordered spins, while SG denotes the spin glass regions. Lines 1, 2, 3 correspond to $n \sim \tilde{n}_0(n_M/n_\gamma)^{1/2}$, $n \sim n_0$, and $n \sim n_0^2/n_\gamma$, respectively.

$p_\sigma = 1/2$ occurs at

$$n \approx (3/2\sqrt{\pi})^6 n_0^2/n_\gamma. \quad (33)$$

The dielectric region is thus bounded from above the parabola (33) and from below by the line $n \sim n_0$. If however $n_0 \gtrsim n > n_M$, then almost all of the electrons leave the donors and enter states in the band, thus giving rise to metallic conduction; moreover, the same is true for impurity levels lying within the threshold region ($\varepsilon_0 \ll \varepsilon_t$). It can be shown that metallic conduction can also occur during incoherent spectral rearrangement when $\tilde{n}_\gamma \gg n \gg n_0$ (and *a fortiori* during coherent rearrangement, since in this case $n \gg \tilde{n}_\gamma \gg n_0$). The regions of metallic phase for $\varepsilon_0 < 0$ and $\varepsilon_0 > 0$ are thus continuously connected. Figure 2 shows the general form of the electron phase state diagram in the variables n, \tilde{n}_0 .

4. IMPURITY SYSTEMS WITH STRONG COULOMB INTERACTION ($\tilde{n}_\gamma \ll n_M$)

In the last section we neglected the Coulomb effects; we will now consider the case when the Coulomb interaction rather than hybridization dominates the behavior of the impurity system. Batyev¹² analyzed a similar problem for $\varepsilon_0 > 0$ in the limit $n_\gamma = 0$; he showed, among other things, that the impurity centers can act as nuclei for three-dimensional Wigner crystallization of charged carriers. Such a system is metallic for impurity concentrations $n > n_M$. We will show below that even weak hybridization ($n_\gamma \ll n_M$) can disrupt the Wigner crystal and cause a transition to the dielectric state.

We first pause to consider the density of the electron states more fully for the case when $n_\gamma = 0$, $\varepsilon_0 > 0$, and $n, n_0 \gg n_M$. Almost all of the impurity centers will then be ionized if $n \ll n_0$. However, if the impurity concentration increases so that $n \gg n_0$, most of the electrons will be trapped, with the remainder $n_0 \ll n$ occupying states in the band. The latter correspond to $n_0 \ll n$ positively charged holes, which repel one another and migrate along the impurity centers to form a Wigner crystal.¹² However, it was shown in Ref. 13 that no true long-range order is established in this case—the regions of crystalline phase are bounded in radius by $r_c \sim a_W(n/n_0)^{4/3} \gg a_W$, where $a_W \sim n_0^{-1/3}$ is the Wigner lattice parameter.

In the absence of hybridization, the density of electron states can be expressed in the form

$$\rho(\varepsilon) = \rho_b(\varepsilon) + \rho_l(\varepsilon), \quad (34)$$

where $\rho_b(\varepsilon)$ and $\rho_l(\varepsilon)$ are the densities of the band states and of the states localized near the impurities, respectively. The band states are appreciably perturbed only near the boundaries of the Brillouin zone of the Wigner crystal. Because their energies are greater than ε_0 , $\rho_b(\varepsilon)$ differs only slightly from $\rho_0(\varepsilon)$ for the energies $\approx \varepsilon_0$ of interest. In the case of Wigner crystallization, the localized state density $\rho_l(\varepsilon)$ has two peaks of widely different areas which are separated by a gap of width $\sim \Delta_c = n_0^{1/3} e^2 / \kappa$ (Δ_c is the characteristic energy scale). The weaker peak, of integrated intensity $\approx n_0$, corresponds to charged impurity centers located at the sites of the Wigner lattice. The position ε'_g of this peak can be found by partitioning the Wigner crystal into Wigner-Seitz spheres. The shift of the peak relative to ε_0 is proportional to the Coulomb potential of the electron at the center of a sphere:

$$\varepsilon'_g = \varepsilon_0 + (9\pi/2)^{1/2} \Delta_c \approx \varepsilon_0 + 2.42 \Delta_c.$$

The discreteness of the impurity centers broadens the peak by an amount $\sim \Delta_c (n_0/n)^{1/3}$. On the other hand, the principal maximum is associated with uncharged impurities and is determined by their local potential distribution. The high-frequency edge of this distribution corresponds to interstitials in the Wigner crystal for which the ionization potential is a minimum; it occurs at the energy

$$\varepsilon_g = \varepsilon_0 + 2[(36\pi)^{1/2} - (64/3)^{1/2}] \Delta_c \approx \varepsilon_0 + 0.43 \Delta_c$$

(for a closely packed cubic lattice). The localized state density $\rho_l(\varepsilon)$ obeys the square-root law

$$\rho_l(\varepsilon) \approx \rho_l'(\varepsilon) = 3 \left(\frac{3}{2\pi} \right)^{1/2} \frac{n}{\Delta_c} \left(\frac{\varepsilon_g - \varepsilon}{\Delta_c} \right)^{1/2}, \quad \varepsilon_g - \varepsilon \ll \Delta_c, \quad (35)$$

for $\varepsilon \approx \varepsilon_g$; $\rho_l(\varepsilon)$ increases to a maximum near ε_0 and then falls off as

$$\rho_l(\varepsilon) \approx \rho_l''(\varepsilon) = 4\pi \frac{n}{\Delta_c} \left(\frac{\Delta_c}{\varepsilon'_g - \varepsilon} \right)^4, \quad (36)$$

for $\varepsilon_g - \varepsilon \gtrsim \Delta_c$. This dependence is of the same form as the behavior of the potential near a Wigner lattice site. The principal peak is thus highly asymmetric and of characteristic width $\sim \Delta_c$.

In order to calculate the position of the Fermi level for this system in the above approximation, we use the corresponding expression

$$E_0 = \langle H \rangle = n\varepsilon_0 + \frac{1}{5\pi^2} \left(\frac{2m}{\hbar^2} \right)^{3/2} \left[\varepsilon_F^{5/2} - \left(\frac{3}{\pi} \right)^{1/2} \varepsilon_F^2 \varepsilon_R^{1/2} - \frac{5}{3} \varepsilon_F^{3/2} \varepsilon_0 \right] \quad (37)$$

for the electron energy of the crystal, where $\varepsilon_R = e^2 m / 2\kappa^2 \hbar^2$. The terms in the right-hand side of (37) correspond respectively to the self-energy of the trapped electrons, the kinetic energy of the electrons in the band states, and the Coulomb energy inside a Wigner-Seitz sphere. The energy (37) has a minimum for

$$\varepsilon_F = \varepsilon_0 + 2/5 (9\pi)^{1/2} \Delta_c \approx \varepsilon_0 + 1.22 \Delta_c, \quad (38)$$

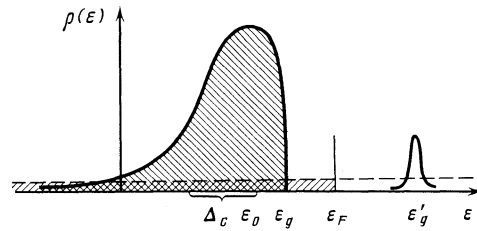


FIG. 3. Density of electron states for $n_\gamma = 0$. The solid curves show $\rho_l(\varepsilon)$, the dashed line gives $\rho_b(\varepsilon)$. The states in the hatched regions are filled.

which as expected lies higher than the edge ε_g of the principal peak and below the edge ε'_g of the secondary peak. Figure 3 shows the general behavior of $\rho(\varepsilon)$.

We will now discuss the effects of hybridization. For $n_\gamma \neq 0$, the indirect hybridization interaction between the impurities gives an additional contribution to $\rho_l(\varepsilon)$, as described by (13). The corresponding states above the Fermi level (38) are not filled, so that a certain number

$$n_p = n'(\varepsilon_F) = \frac{125}{864} \eta_M \frac{n^2 n_\gamma}{n_0 n_M} \quad (39)$$

of the charges are randomly distributed over pairs of neighboring impurities. These charges pin the Wigner lattice, and the radius r_p determines the correlation radius when $r_c > r_p \sim n_p^{-1/3}$ (this situation occurs when $n \gg n_0 (n_M/n_\gamma)^{1/6}$). For $n_p \sim n_0$, however, the correlation radius becomes comparable to the lattice constant, and the Wigner crystal melts completely when $n \sim n_0 (n_M/n_\gamma)^{1/2}$ (this estimate is valid if the hybridization is not too great, i.e., if $n \ll n_0^{4/3} / n_\gamma^{1/3}$, so that ε_0 greatly exceeds the width Δ of the energy interval (11) within which the spectrum changes significantly). The last two conditions are mutually consistent for $n_0 \gg n_M^{3/2} / n_\gamma^{1/2}$; however, if $n_0 < n_M^{3/2} / n_\gamma^{1/2}$ then no Wigner crystallization can occur, at least for $n > n_M^2 / n_\gamma$.

The width Δ of the spectral rearrangement interval becomes comparable to the Coulomb width Δ_c for concentrations $n \sim n_0 (n_M/n_\gamma)^{1/3}$, i.e., even before the Wigner crystal melts. A quasigap of width Δ_c also forms, as discussed in part c) of Sec. 2. Since Δ_c also determines ε_F [Eq. (38)], the Fermi level lies within the quasigap and metal \rightarrow dielectric transition takes place. The same number n_0 of charges will be randomly distributed over pairs of neighboring impurities after the Wigner crystal melts. In this case the secondary peak at $\varepsilon \approx \varepsilon'_g$ disappears. The form of the principal peak is virtually unchanged for $\varepsilon_0 - \varepsilon \gtrsim \Delta_c$; for $\varepsilon - \varepsilon_0 \gg \Delta_c$ the peak has the profile

$$\frac{n}{\Delta_c} \left(\frac{\Delta_c}{\varepsilon - \varepsilon_0} \right)^{1/2} \exp \left[- \frac{(2/\pi)^{1/2}}{3} \left(\frac{\varepsilon - \varepsilon_0}{\Delta_c} \right)^{3/2} \right],$$

while finally, for

$$\varepsilon - \varepsilon_0 \gg \Delta_c \ln^{3/2} (n_0 n_M / n n_\gamma)$$

the peak is described by Eqs. (12), (13). The system may once again become metallic if the donor concentration increases further (cf. Sec. 3), provided that the number $n'(\varepsilon_1)$ of fluctuation states above the edge ε_1 of the upper subband given by (31) exceeds $\max(n_0/2, n_M)$ if $\varepsilon_0 > 0$ [or that $n'(\varepsilon_1) < n_M$ for $\varepsilon_1 < 0$]. The lower boundary of the second metallic region is

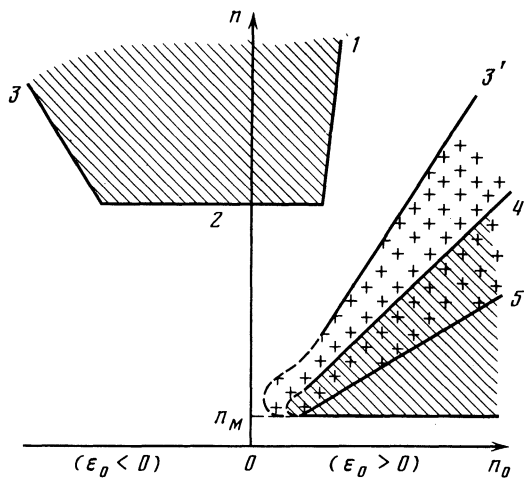


FIG. 4. Phase diagram for $n_\gamma \ll n_M$. The hatched regions correspond to the metallic phase; the crosses (+) show where Wigner crystallization occurs. Lines 1–3 correspond to expressions (40). The other curves are defined as follows: 3') $n_p = n_0$ [cf. (39)]; 4) $n \sim n_0(n_M/n_\gamma)^{1/3}$; 5) $n \approx n_0$.

thus determined by the dependences

$$\begin{aligned} n &= 36\pi n_0^2/n_\gamma, \quad \varepsilon_0 \geq \varepsilon_R, \\ n &= 144\pi n_M^2/n_\gamma, \quad \varepsilon_R \geq \varepsilon_0 \geq -\varepsilon_R/\varepsilon_t^{1/2}, \\ n &= ((3\pi)^3/2)^{1/2} n_0 (n_M/n_\gamma)^{1/2}, \quad \varepsilon_0 \leq -\varepsilon_R/\varepsilon_t^{1/2}. \end{aligned} \quad (40)$$

The above arguments all assume that $\max(n, n_0) \gg n_M$. Other phases (e.g., exciton phases) may form if this condition is violated; however, this goes beyond the scope of the present paper. Figure 4 shows the phase diagram for the electron states described in this section.

5. CONCLUSIONS

The above arguments show that the electronic properties of semiconductor crystals with two-parameter impurity states are much more diverse than for ordinary hydrogen-like impurity states. For example, in addition to the Mott transition, metallic and dielectric phases may alternate if $\varepsilon_0 > 0$ and $n, n_0 > n_M, n_\gamma$ if either the impurity concentration n or the energy ε_0 of the impurity level are varied monotonically

(ε_0 determines the value of n_0). Wigner crystallization and melting may also occur, depending on the values of these parameters. Finally, if $\varepsilon_0 < 0$ and $n_0 \gg n_M$, impurity fluctuation states may produce a metallic phase, and different types of spin ordering (spin glass and ferromagnetic) may alternate.

Systems that exhibit the above behavior include semiconductors with widely different effective masses (so that $n_\gamma \ll n_M$), semiconductors and dielectrics that are suitably doped with transition elements ($n_\gamma \gg n_M$), and many others. Such systems are easily studied by changing the external pressure, magnetic field, or other parameters so as to alter ε_0 or n_0 . Finally, we observe that similar behavior may be anticipated for impurity states generated by intense optical pumping near the edge of the continuous spectrum.

We thank M. A. Krivoglaz for his interest in this work, and A. L. Éfros, B. I. Shklovskii, and M. É. Raïkh for a discussion of several topics touched upon in this paper.

¹N. F. Mott and E. A. Davis, *Electronic Processes in Non-Crystalline Materials*, Clarendon Press, Oxford (1971).

²A. G. Milnes, *Deep Impurities in Semiconductors*, Wiley, New York (1973).

³G. L. Bir, *Fiz. Tverdogo Tela (Leningrad)* **13**, 460 (1971) [*Sov. Phys. Solid State* **13**, 460 (1971)].

⁴M. I. D'yakonov and B. L. Gel'mont, *Zh. Eksp. Teor. Fiz.* **62**, 713 (1972) [*Sov. Phys. JETP* **35**, 377 (1972)].

⁵M. A. Ivanov and Yu. G. Pogorelov, *Zh. Eksp. Teor. Fiz.* **76**, 1010 (1979) [*Sov. Phys. JETP* **49**, 510 (1979)].

⁶P. W. Anderson, *Phys. Rev.* **124**, 41 (1961).

⁷M. A. Ivanov and Yu. G. Pogorelov, *Zh. Eksp. Teor. Fiz.* **72**, 2198 (1977) [*Sov. Phys. JETP* **45**, 1155 (1977)].

⁸A. F. Ioffe and A. R. Regel, *Progr. Semicond.* **4**, 237 (1960).

⁹M. A. Ivanov, V. M. Loktev, and Yu. G. Pogorelov, *Inst. Teor. Fiz. Preprint No. 79-40R*, Kiev (1979).

¹⁰V. M. Naumenko, V. V. Eremenko, V. M. Bandura, and V. V. Pishko, *Pis'ma Zh. Eksp. Teor. Fiz.* **32**, 436 (1980) [*JETP Lett.* **32**, 412 (1980)].

¹¹D. I. Khomskii and A. N. Kocharyan, *Fiz. Tverd. Tela (Leningrad)* **17**, 462 (1975) [*Sov. Phys. Solid State* **17**, 290 (1975)].

¹²É. G. Batyev, *Pis'ma Zh. Eksp. Teor. Fiz.* **29**, 560 (1979) [*JETP Lett.* **29**, 517 (1979)].

¹³M. S. Bello, E. I. Levin, B. I. Shklovskii, and A. L. Éfros, *Zh. Eksp. Teor. Fiz.* **80**, 1596 (1981) [*Sov. Phys. JETP* **53**, 822 (1981)].

Translated by A. Mason